Case Studies in Thermal Engineering 3 (2014) 11–20

Contents lists available at ScienceDirect

Case Studies in Thermal Engineering

journal homepage: www.elsevier.com/locate/csite

The prediction of photovoltaic module temperature with artificial neural networks

İlhan Ceylan [a,*], Okan Erkaymaz [b], Engin Gedik [a], Ali Etem Gürel [c]

[a] Energy Systems Engineering, Technology Faculty, Karabuk University, Karabuk, Turkey
[b] Department of Biomedical Engineering, Engineering Faculty, Bulent Ecevit University, 67100 Zonguldak, Turkey
[c] Department of Electrical and Energy, Duzce Vocational School, Duzce University, Duzce, Turkey

ARTICLE INFO

Article history:
Received 13 December 2013
Accepted 24 February 2014
Available online 6 March 2014

Keywords:
ANN
Photovoltaic
Power
Electrical efficiency

ABSTRACT

In this study, photovoltaic module temperature has been predicted according to outlet air temperature and solar radiation. For this investigation, photovoltaic module temperatures have been determined in the experimental system for 10, 20, 30, and 40 °C ambient air temperature and different solar radiations. This experimental study was made in open air and solar radiation was measured and then this measured data was used for the training of ANN. Photovoltaic module temperatures have been predicted according to solar radiation and outside air temperature for the Aegean region in Turkey. Electrical efficiency and power was also calculated depending on the predicted module temperature. Kütahya, Uşak and Afyon are the most suitable cities in terms of electrical efficiency and power product in the Aegean region in Turkey.

1. Introduction

The solar panels used in photovoltaic systems can be categorized into three groups. These are polycrystalline solar panels, monocrystalline solar panels and amorphous crystal solar panels. Since the production of polycrystalline solar panels commercially is relatively easier, they are the most preferred panels. In addition, they are much cheaper. The efficiency of these three types of solar panels varies from 10% to 20%. Even though the efficiency of polycrystalline solar panels varies in different sources, their efficiency is 15% at the laboratory scale. The efficiency in application could be reduced up to 10%. The biggest loss at solar panels occurs in heating; since it could convert 50% of the solar radiation reflected on it into thermal energy. So it makes solar panels possible to be used in the production of thermal energy. The ANN has been used for predicting different factors of photovoltaic systems. Some of these are listed as below.

Kalogirou et al. [1] used artificial neural networks for the performance prediction of large solar systems. The ANN method is used to predict the expected daily energy output for typical operating conditions, as well as the temperature level of the storage tank can be achieved by the end of the daily operation cycle. Rai et al. [2] developed the simulation model of an ANN based maximum power point tracking controller. The controller consists of an ANN tracker and the optimal control unit. The ANN tracker estimates the voltages and currents corresponding to a maximum power delivered by solar photovoltaic array for variable cell temperature and solar radiation. Karamirad et al. [3] used ANN for predicting photovoltaic panel behaviors under realistic weather conditions. ANN results are compared with analytical four and five

* Corresponding author. Tel.: +90 3704338200.
E-mail address: ilhancey@gmail.com (İ. Ceylan).

http://dx.doi.org/10.1016/j.csite.2014.02.001

Nomenclature

d_k	result expected from layer 2
d_o	error occurred at layer 2
d_y	error occurred at layer 1
E	square error occurred in one cycle
$f(net_i)$	activation function
AE	average error
n	data number
net_i	calculation result of layer 1
net_k	calculation result of layer 2
o_k	result of layer 2
R^2	coefficient of correlation
x_i	input data
w_{ij}	weights in layer 1
w_{jk}	weights in layer 2
y_i	results obtained from layer 1
β	term of momentum
ε	coefficient of approximation
Δw_{jk}	correction made in weights at the previous calculation
Δw_{ij}	correction made in weights at the previous calculation
A	area, m^2
$I(t)$	incident solar intensity, W/m^2
T	temperature, °C
P	power, W

Subscript

c	solar cell
g	glass
m	module
α	absorptivity
δ	packing factor
τ	transmittivity

parameter models of the PV module. Ammar et al. [4] suggested a PV/T control algorithm based on ANN to detect the optimal power operating point (OPOP) by considering PV/T model behavior. The OPOP computes the optimum mass flow rate of PV/T for a considered irradiation and ambient temperature. Mellit et al. [5] described a methodology to estimate the profile of the produced power of a 50 Wp Si-polycrystalline photovoltaic module. For this purpose, two ANNs have been developed for use on cloudy and sunny days. Fernandez et al. [6] proposed a model based on ANNs to predict the maximum power of a High Concentrator Photovoltaic (HCPV) module using easily measurable atmospheric parameters. Almonacid et al. [7] characterized Si-crystalline PV modules by ANNs. An ANN has been developed which can generate *V–I* curves of Si-crystalline PV modules for any irradiance and module cell temperature.

In this study, the module temperature has been predicted to be different from the literature. The main factors determining the module temperature is the ambient air temperature and solar radiation. Module temperatures have been determined in the experimental system for the 10, 20, 30, and 40 °C ambient air temperature and different solar radiations. The experimental study was made in open air and solar radiation was measured and then this measured data was used for the training of ANN. The photovoltaic ambient air temperature is controlled in the experimental system and solar radiation in open air is measured. The module temperature was predicted by ANN depending on the outside temperature and solar radiation for the Aegean region of Turkey.

2. Artificial neural networks

Artificial neural networks (ANNs) are good for some tasks, while lacking in some others. Specifically, they are good for tasks involving incomplete-data sets, fuzzy or incomplete information, and for highly complex and ill-defined problems, where humans usually decide on an intuitional basis. They can learn from examples, and are able to deal with non-linear problems. Furthermore, they exhibit robustness and fault-tolerance. The tasks that ANNs cannot handle effectively are those requiring high accuracy and precision, as in logic and arithmetic [8].

The ANNs are widely used in various fields of mathematics, engineering, meteorology, economics and in adaptive control and robotics, in electrical and thermal load predictions and many other subjects [9]. ANNs show structural and mathematical variations. Structural differences arise from the number of layers and the variations of the connections among the nodes. Generally they have three layers as follows: input layer, hidden layer, and output layer. Number of the layers can change and can be rebounded between the layers. This completely depends on the usage purpose of the network and the design of the designer. Number of nodes in the input layer is equal to the number of data given to ANN. Number of nodes at the output layer is equal to the number of knowledge that will be taken from ANN. Node number of the hidden layer is found experimentally. Learning capability of ANN improves as the number of nodes and the connections increase; however, it takes more time to train ANN. A node has many inputs whereas it has only one output. Nodes process these input data and feeds forward to the next layer. Input data are processed as follows: each data was added up after it was multiplied by its weight and then it was subjected to activation function. Thus the data which will be transferred to the next layer is obtained [10].

The algorithm used in training ANN and the type of activation function used at the output of the node are the mathematical differences. Activation functions involve exponential functions and thus non-linear modeling can be achieved.

Various algorithms have been developed according to the ANNs' purpose of usage. They can be preferred according to their convenience to the problem to be solved, and training speed.

ANNs are trained with known data and then tested with data not used in training. Although training takes a long time, they make decisions very fast during operation.

They are used widely in modeling non-linear systems, thanks to their ability to learn, to generalize, to tolerate the faults and to benefit from the faulty samples [11].

"Back propagation algorithm", which optimizes the weighted connections by allowing the error to spread from output layer towards the lower layers, was used as the training system in training networks. This algorithm is the most widely used method in artificial neural networks.

The formulas used in this algorithm are as follows:

Hidden layer calculation results

$$net_i = \sum x_i w_{ij} \tag{1}$$

$$y_i = f(net_i) \tag{2}$$

Output layer calculation results

$$net_k = \sum y_i w_{jk} \tag{3}$$

$$o_k = f(net_k) \tag{4}$$

Activation function used in both layers

$$f(net_i) = 1/(1+e^{-net}) \tag{5}$$

Errors made at the end of one cycle

$$d_o = (d_k - o_k) o_k (1 - o_k) \tag{6}$$

$$d_y = y_i (1 - y_i) \sum d_o w_{ij} \tag{7}$$

Weights can be changed using these calculated error values according to the following formulas [10]:

$$w_{jk} = w_{jk} + \varepsilon d_o y_i + \beta \Delta w_{jk} \tag{8}$$

$$w_{ij} = w_{ij} + \varepsilon d_y x_i + \beta \Delta w_{ij} \tag{9}$$

Values between 0.1 and 0.9 are proposed for the coefficient of approximation (ε) and term of momentum (β) [12].

Square error, occurred in one cycle, can be found by the following equation:

$$e = \sum 1/2 |d_k - o_k|^2 \tag{10}$$

In an ANN, the number of inputs cells is equal to the number of data at input, and the output cell number equals to the number of data taken from the output. Some equations were given for the hidden cell number but it is generally found by the trial and error method. The following equation was proposed for the hidden cell number:

$$\text{Number of hidden cells } 1/2\ (\text{inputs} + \text{outputs}) + \sqrt{\text{number of training data}} \tag{11}$$

Following the completion of training ANN, average error (AE) for all data are calculated according to the following formula for the testing network [13,14]:

$$(AE) = \frac{1}{n} \sum_{i=1}^{n} \left(\frac{100(d_k - o_k)}{d_k} \right) \tag{12}$$

3. Experimental setup

The experimental system is shown in Fig. 1. Photovoltaic ambient air temperature was controlled in this system for 10 °C, 20 °C, 30 °C, and 40 °C temperatures. The system consisted of cooling and heating systems. The cooling system contained a compressor, condenser, evaporator, fan, dryer and capillary tube. Also the heating system consisted of an electrical heater with controlled process control equipment as a selecting PID section. When the photovoltaic module ambient air temperature was controlled by the outside placed experimental system, solar radiation and photovoltaic module back-side temperature could be measured. The measured and adjusted module ambient air temperatures are shown in Fig. 2.

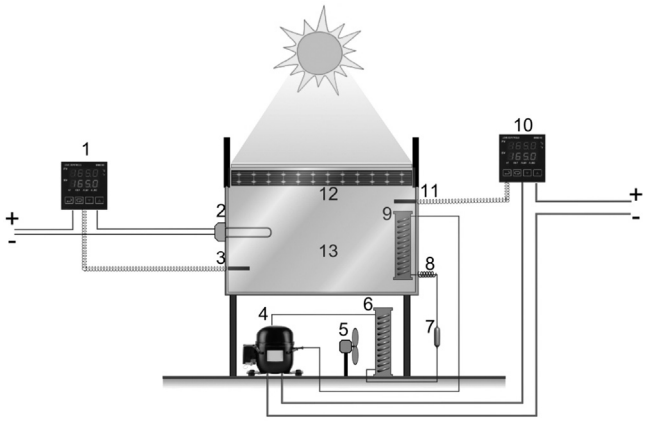

Fig. 1. The experimental system. 1. Process control equipment (for heater). 2. Electrical heater. 3. Temperature sensor. 4. Compressor. 5. Fan. 6. Condenser. 7. Dryer. 8. Capillary tube. 9. Evaporator. 10. Process control equipment (for refrigerator). 11. Temperature sensor. 12. Photovoltaic module.

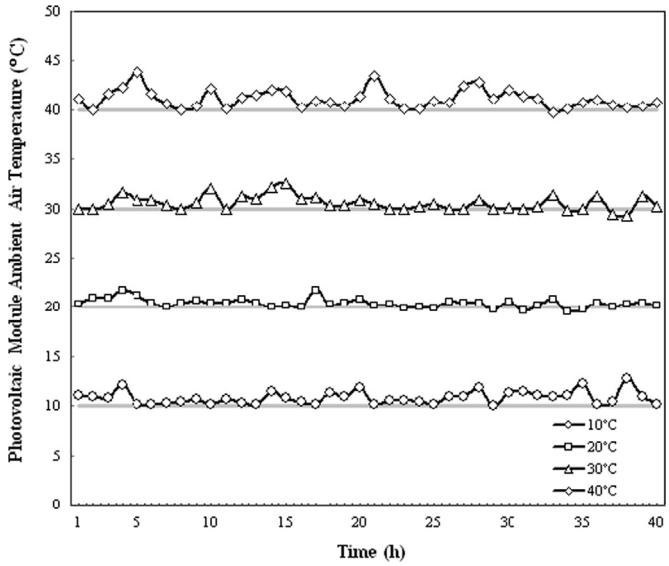

Fig. 2. Measured and adjusted photovoltaic module ambient air temperatures.

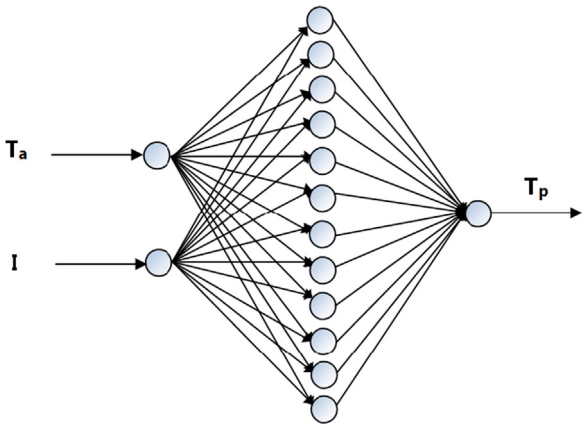

Fig. 3. Neural network structure.

4. Energy analysis of photovoltaic module

It is possible to analyze the electrical efficiency of the photovoltaic panels in two categories as module and cell efficiency. The highest electrical loss of the panels occurs with temperature. Open circuit voltage and fill factor decrease significantly with temperature. But nonetheless, short circuit current increases for a while [15,16]. At the end of this common effect, electrical efficiency is calculated as follows:

$$\eta_c = \eta_0[1-\beta(T_c-25)] \tag{13}$$

where η_0 is the efficiency at standard test conditions ($I(t)=1000\ \mathrm{W/m^2}$, $T_c=25\ ^\circ\mathrm{C}$), T_c is the solar cell temperature and β is the electrical efficiency thermal coefficient.

β value depends on the features of the materials from which the PV module is produced. For crystal silicon almost 0.0045/K is taken, 0.0035/K is taken for CIS, 0.0025/K for CdTe and 0.002/K for a-Si [15,17].

	Samples	MSE	R
Training:	177	9.39297e-4	9.91916e-1
Validation:	24	2.05824e-3	9.84776e-1
Testing:	36	1.69958e-3	9.86689e-1

Fig. 4. Training performance.

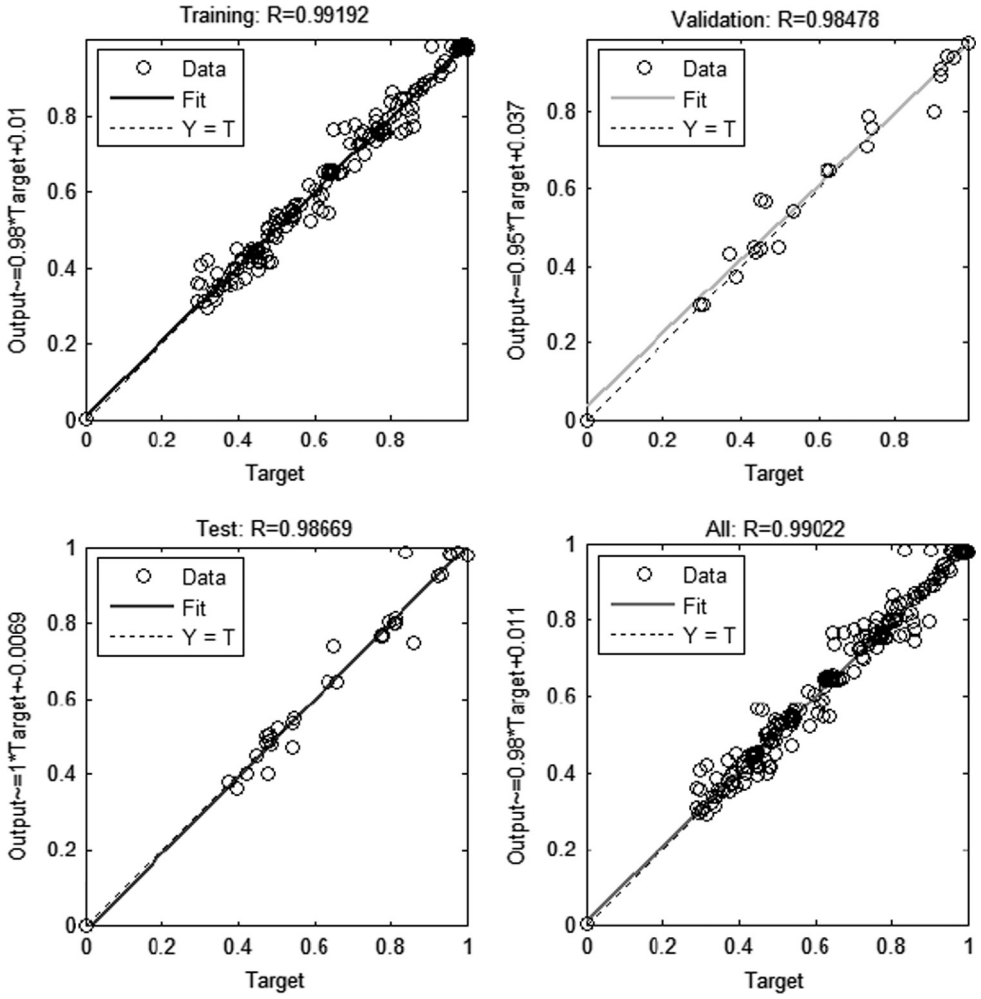

Fig. 5. Regression analysis of training process.

In addition, the electrical efficiency of the PV module is given as follows:

$$\eta_m = \eta_c \tau_g \alpha_c \delta_c \tag{14}$$

where τ_g is the transparency for the PV module glass, α_c is the absorptivity of the solar cell and δ_c is the packing factor; the values for these are taken as 0.90, 0.95 and 0.90, respectively [15,18].

Another expression of the module efficiency can be written as follows:

$$\eta_m = \frac{P}{A_m I(t)} \tag{15}$$

The output power P of the PV module is calculated using the measured voltage and current values as follows:

$$P = VI \tag{16}$$

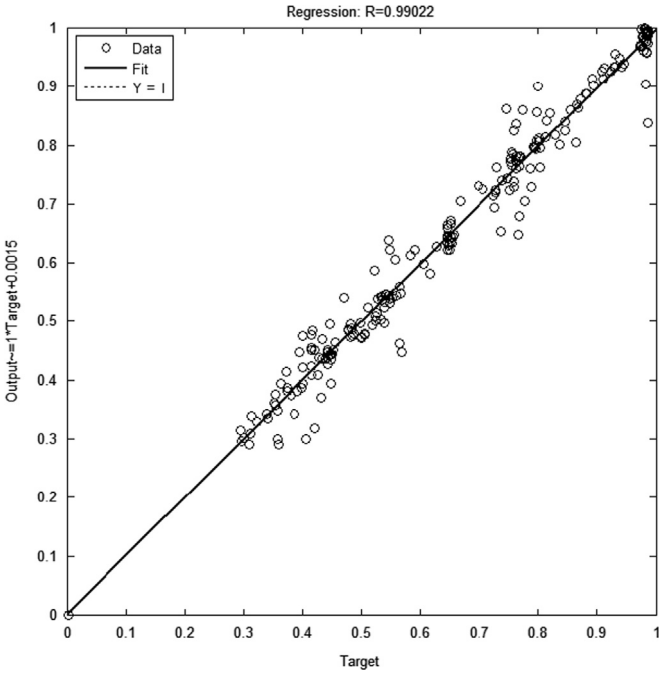

Fig. 6. Test phase perform.

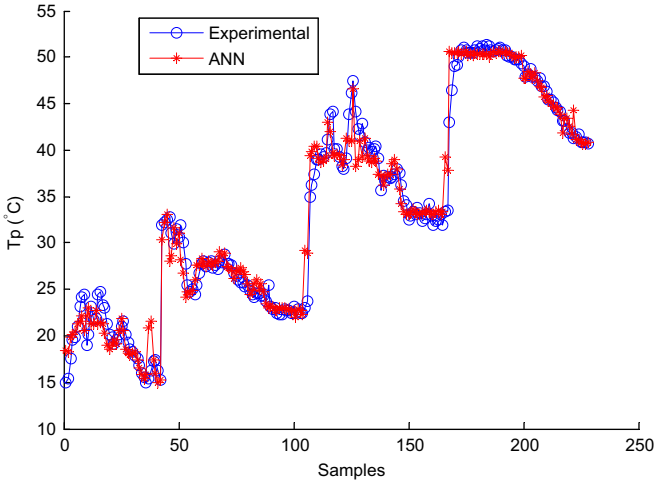

Fig. 7. The predicted (with ANN) and experimental variables.

The electrical energy gain obtained from the PV module can be calculated as follows:

$$\dot{E}_{l,net\ \ electrical} = \eta_m A_m I(t) \tag{17}$$

where η_m is the module efficiency and A_m is the module surface area.

5. Result and discussion

Photovoltaic module ambient air temperatures were attempted to be maintained at 10 °C, 20 °C, 30 °C and 40 °C in the system. The change in module ambient air temperatures according to experimental time is shown in Fig. 2. While, the solar radiation from top of the module and module back side temperature were measured in the experimental system. Controlled photovoltaic module ambient air temperature and measured solar radiation were used for ANN as input variables. Also the measured module back side temperatures were used as output variables in the ANN.

In this study, a three-layer feed-forward neural network was used. The Levenberg–Marquardt back-propagation method was selected as the learning algorithm. The proposed three layers network structure is shown in Fig. 3. In this structure,

Table 1
Monthly average daily solar radiation values of the Aegean region of Turkey (W/m^2).

	Jan.	Feb.	March	April	May	June	July	Aug.	Sept.	Oct.	Nov.	Dec.
İzmir	372.43	368.6	544.54	621.42	607.98	546.68	513.93	501.74	478.8	465.18	396.4	379.39
Denizli	411.88	426.09	599.12	665.82	645.23	592.43	559.59	536.19	512.85	510.2	426.02	423.17
Manisa	386.96	403.66	573.82	650.92	625.92	568.9	534.41	517.18	500	485.23	408.05	398.48
Kütahya	477.09	493.72	681.81	741.35	682.38	629.74	592.39	566.9	526.97	523.96	429.47	430.2
Aydın	385.66	384.62	572.86	640.3	617.83	560.65	525.23	517.03	493.4	491.53	413.19	402.25
Uşak	397.83	452.16	608.36	680.48	654.42	607.57	580.56	546.47	514.93	506.49	426.07	414.57
Muğla	411.31	390.32	595.51	660.15	627.65	580.56	543.7	534.92	509.07	504.46	425.96	402.57
Afyon	473.15	477.76	709.22	723.4	669.9	619.05	591.55	553.59	523.96	517.59	427.73	443.85

Table 2
Monthly average outside air temperature of the Aegean region of Turkey (°C).

	Jan.	Feb.	March	April	May	June	July	Aug.	Sept.	Oct.	Nov.	Dec.
İzmir	8.8	9.4	11.7	15.9	20.9	25.7	28	27.6	23.6	18.9	14.1	10.6
Denizli	5.8	6.9	10	14.6	19.7	24.7	27.4	26.9	22.4	16.8	11.4	7.6
Manisa	6.7	7.9	10.7	15.2	20.5	25.5	28.1	27.7	23.4	18	12.2	8.5
Kütahya	0.4	1.7	5.2	10	14.6	18.4	20.9	20.6	16.6	11.8	6.7	2.6
Aydın	8.1	9.2	11.8	15.8	20.9	25.9	28.4	27.4	23.3	18.4	13.3	9.6
Uşak	2.3	3	6.3	10.8	15.8	20.3	23.6	23.4	19	13.4	8	4.2
Muğla	5.5	6	8.6	12.5	17.6	22.9	26.3	26	21.7	16	10.5	7
Afyon	0.2	1.5	5.4	10.3	15	19.1	22.3	22	17.8	12.3	6.8	2.5

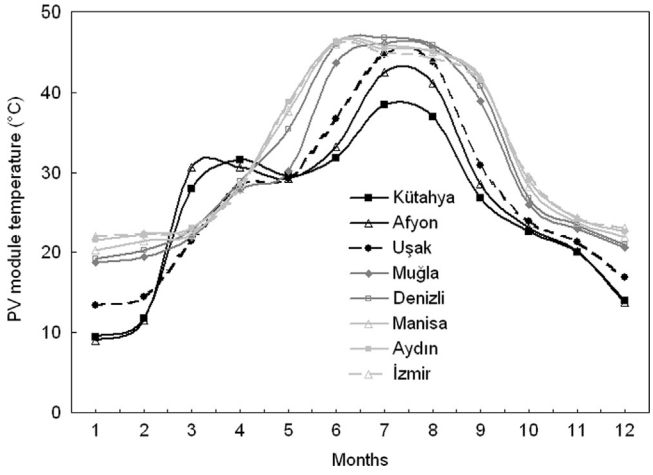

Fig. 8. Predicted photovoltaic module temperature with ANN.

measured solar radiation (I) and controlled module ambient air temperatures (T_a) were used as two input variables. Photovoltaic module back side temperatures (T_p) were used as the output variable. The number of neuron in hidden layer was defined as 12 with trials and 228 samples dataset were used in matlap neural networks tool in order to train and predict. In training phase, the 10 fold cross-validation method was used to solve over the fitting problem. While 80% of dataset was used for training, 10% was used for validation and 15% was used for test process. Mean square error (MSE) parameter was used to stop the training process and training process results are shown in Fig. 4. Regression analysis of training process is also given in Fig. 5.

Tested network using whole dataset and results is shown in Fig. 6. Network test error was obtained as 1.16016e-3 and regression coefficient (R) obtained as 9.90215e-1. As a result, prediction of ANN and experimental data were compared with each other and shown in Fig. 7.

After test and training process of experimental values, photovoltaic module temperatures were predicted with ANN depending on outlet air temperature and solar radiation of Aegean region in Turkey. The used outlet air temperature and solar radiation are shown in Tables 1 and 2. The predicted photovoltaic module temperature using ANN is also shown in

Table 3
Predicted back side temperature of the photovoltaic module (°C).

	Jan.	Feb.	March	April	May	June	July	Aug.	Sept.	Oct.	Nov.	Dec.
İzmir	22	22.4	22.6	28	38.7	46	45	44.3	41.4	29.5	24.4	23.1
Denizli	19.2	20.3	22.9	28.9	35.4	46	46.8	45.9	40.8	26.8	23.4	21
Manisa	20.3	21.4	22.3	28.6	37.6	46.4	45.9	45.1	42	28.2	23.8	21.9
Kütahya	9.4	11.8	28	31.6	29.6	31.8	38.5	37	26.8	22.6	20.1	14
Aydın	21.6	22.3	23.1	28.6	38.8	46.4	45.5	45.1	41.6	29	24.2	22.6
Uşak	13.4	14.5	21.4	28.4	29.2	36.7	44.8	43.8	30.9	23.9	21.3	16.9
Muğla	18.8	19.5	21.9	27.8	30.2	43.7	46.1	45.6	38.9	26	23	20.6
Afyon	9	11.5	30.7	30.7	29.3	33.2	42.5	41.1	28.5	23.1	20.2	13.7

Table 4
Calculated electrical efficiency of photovoltaic module (%).

	Jan.	Feb.	March	April	May	June	July	Aug.	Sept.	Oct.	Nov.	Dec.
İzmir	11.7	11.68	11.67	11.39	10.83	10.45	10.50	10.54	10.69	11.31	11.57	11.64
Denizli	11.84	11.79	11.65	11.34	11	10.45	10.41	10.46	10.72	11.45	11.63	11.75
Manisa	11.79	11.73	11.68	11.36	10.89	10.43	10.46	10.5	10.66	11.38	11.60	11.70
Kütahya	12.35	12.23	11.39	11.20	11.30	11.19	10.84	10.92	11.45	11.69	11.80	12.11
Aydın	11.72	11.68	11.64	11.35	10.83	10.43	10.48	10.5	10.68	11.34	11.58	11.67
Uşak	12.14	12.09	11.73	11.37	11.32	10.94	10.51	10.57	11.24	11.60	11.73	11.96
Muğla	11.86	11.83	11.7	11.40	11.27	10.57	10.45	10.47	10.82	11.49	11.65	11.77
Afyon	12.37	12.24	11.25	11.25	11.32	11.12	10.63	10.71	11.36	11.64	11.79	12.13

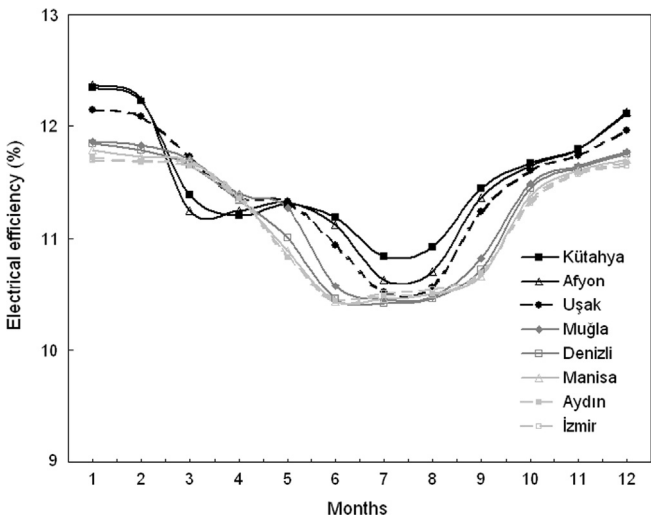

Fig. 9. Calculated photovoltaic module electrical efficiency.

Table 5
Calculated power of photovoltaic module (W/m^2).

	Jan.	Feb.	March	April	May	June	July	Aug.	Sept.	Oct.	Nov.	Dec.	Total
İzmir	43.57	43.04	65.53	70.76	65.85	57.14	53.98	52.88	51.19	52.61	45.88	44.16	644.59
Denizli	48.78	50.22	69.81	75.50	70.99	61.92	58.25	56.07	54.99	58.41	49.53	49.72	704.20
Manisa	45.61	47.35	67.04	73.92	68.15	59.34	55.88	54.30	53.30	55.20	47.35	46.64	674.07
Kütahya	58.93	60.37	77.64	83.03	77.13	70.46	64.22	61.90	60.33	61.13	50.66	52.11	777.93
Aydın	45.20	44.93	66.69	72.71	66.88	58.48	55.03	54.28	52.70	55.71	47.86	46.93	667.41
Uşak	48.32	54.66	71.36	77.34	74.11	66.44	61.04	57.74	57.86	58.75	50	49.60	727.20
Muğla	48.80	46.17	69.70	75.24	70.75	61.37	56.80	56.02	55.08	57.96	49.61	47.39	694.89
Afyon	58.55	58.49	79.76	81.36	75.83	68.82	62.90	59.27	59.53	60.25	50.44	53.84	769.03

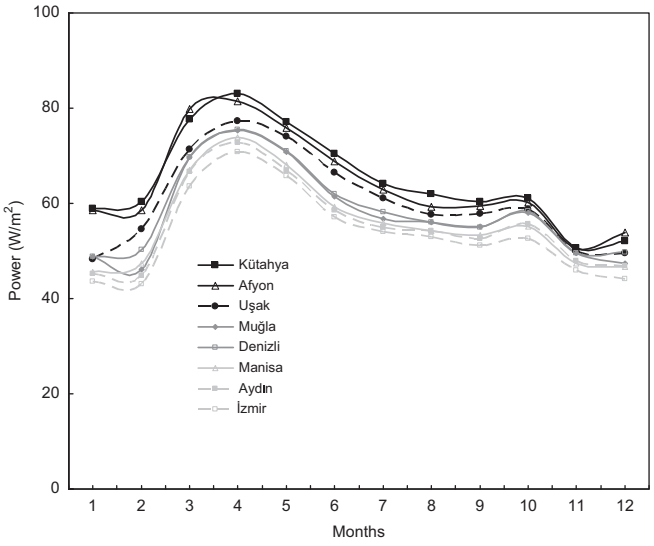

Fig. 10. Calculated photovoltaic module power.

Fig. 8 and Table 3. As can be seen in Fig. 8, Kütahya city has the lowest module temperature. Using these predicted values, electrical efficiency was calculated from Eqs. (13) and (14). The calculated electrical efficiency for each city is shown in Fig. 8 and Table 4. The calculated electrical efficiency was used in Eq. (15) and photovoltaic power per square meter for each city was calculated. As can be seen from Fig. 8, as the solar radiation increased, the photovoltaic module temperature increased. The lowest module temperatures were predicted for Kütahya, Afyon and Uşak cities.

The calculated photovoltaic module power is shown in Fig. 9 and Table 5 for each city of Aegean region in Turkey. Despite the high solar radiation for these cities, module temperature was predicted as lower. Consequently, these cities' electrical efficiency was higher, as calculated from Eqs. (13) and (14). This situation can be seen from Fig. 9. As can be seen in Fig. 9, electrical efficiency was low in 6th, 7th, and 8th months despite solar radiation being high in these months. March, April and May shows both high solar radiation and low module temperature according to Tables 1 and 3. Thus, high solar radiation and low module temperature can be inferred from high power product.

6. Conclusion

The measured, calculated and predicted values obtained from the results of this study are discussed as follows:

1. The outside air temperature is a very important factor in terms of photovoltaic module temperature. As can be seen in Tables 2 and 3, outside air temperature can be compared with predicted module temperature.
2. As the solar radiation increased, photovoltaic module electrical efficiency decreased according to Figs. 8 and 9. However, the power of photovoltaic module increased as the solar radiation increased.
3. Photovoltaic module temperature was the highest predicted for İzmir city, but the lowest temperature was predicted for Kütahya city. At the same time Kütahya city has the highest solar radiation value and the lowest outside air temperature; this situation can be seen in Tables 1 and 2.
4. As can be seen in Fig. 10, the highest power was predicted between the third and seventh months for all cities.

References

[1] Kalogirou SA, Mathioulakis E, Belessiotis V. Artificial neural networks for the performance prediction of large solar systems. Renew Energy 2014;63:90–7.
[2] Rai AK, Kaushika ND, Singh B, Agarwal N. Simulation model of ANN based maximum power point tracking controller for solar PV system. Sol Energy Mater Sol Cells 2011;95:773–8.
[3] Karamirad M, Omid M, Alimardani R, Mousazadeh H, Heidari SN. ANN based simulation and experimental verification of analytical four- and five-parameters models of PV modules. Simul Model Pract Theory 2013;34:86–98.
[4] Ammar MB, Chaabene M, Chtourou Z. Artificial neural network based control for PV/T panel to track optimum thermal and electrical power. Energy Convers Manag 2013;65:372–80.
[5] Mellit A, Sağlam S, Kalogirou SA. Artificial neural network-based model for estimating the produced power of a photovoltaic module. Renew Energy 2013;60:71–8.
[6] Fernandez EF, Almonacid F, Rodrigo P, Perez-Higueras P. Model for the prediction of the maximum power of a high concentrator photovoltaic module. Sol Energy 2013;97:12–8.
[7] Almonacid F, Rus C, Hontoria L, Munoz FJ. Characterisation of PV CIS module by artificial neural networks. A comparative study with other methods. Renew Energy 2010;35:973–80.
[8] Ceylan I, Aktaş M. Modeling of a hazelnut dryer assisted heat pump by using artificial neural networks. Appl Energy 2008;85:841–54.
[9] Koca A, Oztop HF, Varol Y, Koca GO. Estimation of solar radiation using artificial neural networks with different input parameters for Mediterranean region of Anatolia in Turkey. Expert Syst Appl 2011;38:8756–62.
[10] Yılmaz S, Atik K. Modeling of a mechanical cooling system with variable cooling capacity by using artificial neural network. Appl Therm Eng 2007;27:2308–13.
[11] Kalogirou SA. Applications of artificial neural networks in energy systems: a review. Energy Convers Manag 1999;40:1073–87.
[12] Soteris K, Bojic M. Artificial neural networks for the prediction of the energy consumption of a passive solar building. Energy 2000;25:479.
[13] Genel K, Kurnaz SC, Durman M. Modeling of tribologial properties of alumina fiber reinforced zinc–aluminum composites using artificial neural network. Mater Sci Eng 2003;363:203.
[14] Islamoglu Y, Kurt A. Heat transfer analysis using ANNs with experimental data for air flowing through corrugated channels. Int J Heat Mass Transf 2004;47:1361.
[15] Mishra RK, Tiwari GN. Energy and exergy analysis of hybrid photovoltaic thermal water collector for constant collection temperature mode. Sol Energy 2013;90:58–67.
[16] Zondag HA. Flat-plate PV-Thermal collectors and systems: a review. Renew Sustain Energy Rev 2008;12(4):891–959.
[17] Tiwari GN, Dubey S. Fundamentals of photovoltaic modules and their applications. United Kingdom: RSC Publishing; 2010.
[18] Dubey S, Solanki SC, Tiwari A. Energy and exergy analysis of PV/T air collectors connected in series. Energy Build 2009;41:863–70.